First-principles study of electron transport through monatomic Al and Na wires

Nobuhiko Kobayashi

RIKEN (The Institute of Physical and Chemical Research), 2-1 Hirosawa, Wako, Saitama 351-0198, Japan

Mads Brandbyge

Mikroelektronik Centret (MIC), Technical University of Denmark, Building 345E, DK-2800 Lyngby, Denmark

Masaru Tsukada

Department of Physics, Graduate School of Science, University of Tokyo, 7-3-1 Hongo, Bunkyo-ku, Tokyo 113-0033, Japan

We present first-principles calculations of electron transport, in particular, the conduction channels of monatomic Al and Na atom wires bridged between metallic jellium electrodes. The electronic structures are calculated by the first-principles recursion-transfer matrix method, and the conduction channels are investigated using the eigenchannel decomposition (ECD) of the conductance, the local density of states (LDOS), and the current density. The ECD is different from the conventional decomposition of atomic orbitals, and the study of decomposed electronic structures is shown to be effective in clarifying the details of transport through atomic wires. We show channel transmissions, channel resolved LDOS, and channel resolved current density, and elucidate the number of conduction channels, the relation between atomic orbitals and the channels, and their dependency on the geometry of the atomic wire. We demonstrate that stretching of the bent wire can explain the mechanism of the increase of conductance of Al during the elongation of the contacts. The behavior of our calculated conductance and channel transmissions during the stretching process is in good agreement with the experimental data.

I. INTRODUCTION

Atomic scaled point contacts have been formed by experimental techniques such as scanning tunneling microscopy[1] (STM) and mechanically controllable break (MCB) junctions,[2] and intensive efforts have been made to investigate electron transport through the contacts.[3–31] In the early stage of investigations into the conductance of atomic-scale systems, a central question was whether the quantized conductance ($G_0 = 2e^2/h$) observed in two-dimensional electron gases[32,33] was really observed or not. The atomic configuration is significantly rearranged when the conductance changes abruptly.[5] Nevertheless, clear sharp peaks at the quantized value have been observed in the conductance histograms, particularly for s-valence materials. To clarify the experimental results, various theoretical approaches have been applied.[34–54]

In the last few years, not only the conductance but also individual conduction channels, which are important in order to understand quantum transport through narrow systems, have been investigated using superconducting-normal-superconducting (SNS) junctions.[55,56] From a theoretical viewpoint the concept of eigenchannels[57] has been utilized for model potentials,[58–60] in tight binding model calculations,[61–63] and for the potentials derived from the self-consistent potentials obtained in electronic structure calculations.[64,65]

In this paper, we present first-principles calculations of electron transport, in particular, the conduction channels through Al and Na atom wires, using the eigenchannel decomposition (ECD) combined with the first-principles recursion-transfer matrix (RTM) method.[66] The electronic states are calculated using the first-principles RTM method,[67] and conductance, local density of states (LDOS), and current density[68] are decomposed into eigenchannels. We calculate the eigenchannels from the wave functions obtained self-consistently. Since the eigenchannels are investigated using plane waves which form a complete basis set, the number of channels is not limited to that of the valence electrons. Our calculations enable us to discuss the dependency of the electron transport upon changes of the atomic configurations. Channel resolved electronic structures, particularly channel resolved LDOS and current density, prove to be effective and allow an intuitive understanding of the electron transport. We show them for Al and Na atom wires.

Thus far, to the best of our knowledge a first-principles study of the conduction channels of atomic scale Al contacts has not been performed, although interesting phenomena have been observed experimentally, that is, more than one channel contributes to the transport through a single atom contact,[55] and the conductance staircases show positive slopes during the elongation processes.[7,40,62] We calculate the number of contributing conduction channels, and elucidate the relation between the atomic orbitals and the channels, and their dependency on the geometry of the atomic wire. In our previous proceedings,[69] we reported the effect of slight bending of the wires using a model consisting of only three atoms between jellium electrodes. Here, we consider the three-atom wires with additional atomic bases between the jellium electrodes to reduce the effect of the jellium electrodes. Using the model, we investigate the effect of more bending structures through the straight structure corresponding to a wider range of electrode spacing. In addition, we also discuss the effect of the elongation of the bonds. We
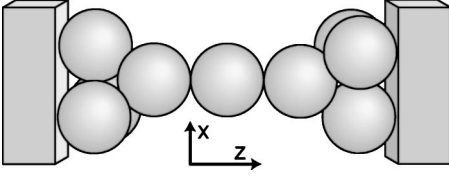
FIG. 1. Schematic representation of the model used.

compare our calculated results with experimental data, and show that stretching of the bent wire can explain the mechanism of the positive slope of the conductance of Al. We find that the behavior of our calculated conductance and channel transmissions in the stretching process is in good agreement with the experimental data.

The paper is organized as follows: First, we describe how the ECD analysis can be performed on the conductance, LDOS, and current density in combination with the RTM method. Then we report the results of an ECD analysis of RTM calculations for Al/Na monatomic wire structures with the focus on the effects of geometrical changes. Finally, we compare these results and conclude.

II. RTM-ECD METHOD

Our investigation of electronic transport through the atomic wires is based on the density functional theory within the local density approximations.[70] Electronic states are calculated by the RTM method,[67] and the electronic states are decomposed into a sum over conduction channels with ECD. In particular, the conductance, the LDOS, and the current density[68] are decomposed into eigenchannels.

We consider a model consisting of an atomic wire sandwiched between two semi-infinite metallic jellium electrodes as shown in Fig. 1. The density of the jellium electrodes ρ_+ is expressed as the commonly used r_s parameter which satisfies

$$\frac{4}{3}\pi r_s^3 \rho_+ = 1. \qquad (1)$$

A supercell structure is taken in the x and y directions. The x and y axes are set laterally to the jellium electrode surface and the z axis is set in the direction normal to the jellium surface.

The Hamiltonian of the system is written as follows:

$$\mathcal{H} = -\frac{\hbar^2}{2m}\nabla^2 + V_{\mathrm{eff}}(\boldsymbol{r}). \qquad (2)$$

The effective potential $V_{\mathrm{eff}}(\boldsymbol{r})$ is calculated as a sum of the ion-core potentials, the Hartree potential, and the exchange-correlation potential in the self-consistent calculations within the local density approximation:

$$V_{\mathrm{eff}}(\boldsymbol{r}) = V_{\mathrm{ion}}(\boldsymbol{r}) + V_{\mathrm{h}}(\boldsymbol{r}) + V_{\mathrm{xc}}[\rho(\boldsymbol{r})]. \qquad (3)$$

Electronic states in the system are written as a sum of the states incident from left and right. They are expressed as scattering plane waves in multichannels, $\boldsymbol{\Psi}^{L(R)}(\boldsymbol{r})$, which consist of a set of wave functions $\Psi_m(\boldsymbol{r})$ incident from channels m:

$$\boldsymbol{\Psi}^{L(R)}(\boldsymbol{r}) = [\Psi_1(\boldsymbol{r}), \Psi_2(\boldsymbol{r}), \ldots, \Psi_N(\boldsymbol{r})]. \qquad (4)$$

The wave function Ψ_m is expanded using plane waves in the x and y directions in the Laue representation

$$\Psi_m(\boldsymbol{r}) = e^{i\boldsymbol{k}_\parallel \cdot \boldsymbol{r}_\parallel} \sum_{n=1}^{N} \psi_{nm}(z) e^{i\boldsymbol{G}_\parallel^n \cdot \boldsymbol{r}_\parallel}, \qquad (5)$$

where $\boldsymbol{G}_\parallel^n$ is a set of two-dimensional reciprocal lattice vectors in the $\boldsymbol{r}_\parallel = (x,y)$ direction. The coefficient matrix $\psi_{nm}(z)$ is solved using the RTM equation[67] and the wave functions are obtained.

The actual number N of plane waves for a given $\boldsymbol{k}_\parallel$ is limited by the cutoff energy E_{cut}, which is increased until the results have converged to the required accuracy

$$\frac{\hbar^2}{2m}|\boldsymbol{k}_\parallel + \boldsymbol{G}_\parallel^n|^2 \leq E_{\mathrm{cut}} \quad (n=1,2,\ldots,N). \qquad (6)$$

For high enough cutoff energy the wave functions within the unit cell localize around the atoms and the jellium electrodes, and vanish in the vacuum region as will be seen in the calculated results. Furthermore, we ensure that our results for the electronic transport do not change significantly when we increase size of the unit cell in the x and y directions, i.e., there is no significant interaction between the periodically repeated wires.

The electron density is obtained as

$$\rho(\boldsymbol{r}) = \frac{m}{\pi \hbar^2} \sum_{L,R} \int dE$$
$$\times \mathrm{tr}\left(\int d\boldsymbol{k}_\parallel [\boldsymbol{\Psi}^{L(R)}(\boldsymbol{r})\mathbf{k}_z^{-1/2}]^\dagger [\boldsymbol{\Psi}^{L(R)}(\boldsymbol{r})\mathbf{k}_z^{-1/2}] \right). \qquad (7)$$

Here, $\mathbf{k}_z^\beta$ is an $N \times M$ rectangular matrix whose nm elements are given by

$$(\mathbf{k}_z^\beta)_{nm} = \delta_{nm}[\sqrt{(2m/\hbar^2)(E - V_{L(R)}) - |\boldsymbol{k}_\parallel + \boldsymbol{G}_\parallel^n|^2}]^\beta, \quad (8)$$

and M is the number of open channels deep in the electrode on the left (right). We do not explicitly write the index L or R on $\mathbf{k}_z$ when it appears together with $\boldsymbol{\Psi}^{L(R)}$.

The Hartree potential is calculated using the Poisson equation, and the exchange-correlation potential is obtained by the local density approximation. Thus, the electronic states are calculated self-consistently.

Conductance per unit cell is calculated with the transmission matrix $\mathbf{T}$ as

$$G(E) = \frac{2e^2}{h} \int d\boldsymbol{k}_\parallel \frac{S}{(2\pi)^2} \mathrm{tr}(\mathbf{T}^\dagger \mathbf{T}), \qquad (9)$$

where S is the area of the unit cell in the x and y directions. In the case of a large supercell compared with the size of the wire, we can use only the Γ point, $\boldsymbol{k}_\parallel = (0,0)$, for the transmission properties. In such a case, the conductance formula is simply the Landauer formula

$$G(E) = \frac{2e^2}{h} \mathrm{tr}(\mathbf{T}^\dagger \mathbf{T}). \qquad (10)$$

The Hermitian matrix $\mathbf{T}^\dagger\mathbf{T}$ is diagonalized using a unitary matrix $\mathbf{U}$ to transform the original channels into eigenchannels, and we obtain eigenchannel transmissions T_i,

$$\mathbf{U}^\dagger\mathbf{T}^\dagger\mathbf{T}\mathbf{U}=\mathrm{diag}\{T_i\}. \tag{11}$$

The eigenchannels form a complete orthogonal set with well defined transmissions, i.e., without interchannel scattering. The LDOS and the current density can be expressed using the eigenchannel basis.[68] The eigenchannel resolved LDOS and the eigenchannel resolved current density are respectively written as

$$\rho^{L(R)}_{E,n}(\boldsymbol{r})=\frac{4\pi m}{h^2}\frac{1}{S}([\boldsymbol{\Psi}^{L(R)}(\boldsymbol{r})\mathbf{k}_z^{-1/2}\mathbf{U}]^\dagger[\boldsymbol{\Psi}^{L(R)}(\boldsymbol{r})\mathbf{k}_z^{-1/2}\mathbf{U}])_{nn},$$
$$\tag{12}$$

$$\boldsymbol{j}^{L(R)}_{E,n}(\boldsymbol{r})=\frac{2e^2}{h}\frac{1}{S}$$
$$\times\mathfrak{I}([\boldsymbol{\Psi}^{L(R)}(\boldsymbol{r})\mathbf{k}_z^{-1/2}\mathbf{U}]^\dagger\nabla[\boldsymbol{\Psi}(\boldsymbol{r})^{L(R)}\mathbf{k}_z^{-1/2}\mathbf{U}])_{nn}.$$
$$\tag{13}$$

Clearly the eigenchannel LDOS and the eigenchannel current density summed over channels yield the total LDOS and the total current density, since this summation corresponds to the invariant trace of a matrix. Hereafter we call the eigenchannel ''conduction channel'' or ''channel,'' and the eigenchannel resolved transmission/LDOS/current density ''channel transmission/LDOS/current density.''

In the numerical calculations, the side lengths of the supercell in the x and y directions are 20 bohrs and the cutoff energy for plane waves is 4 (3) Ry for Al (Na). The mesh size in the z direction is taken to be 0.45 (0.5) bohrs. The r_s parameter for the jellium electrodes is taken to be 2 (4) bohrs. The same Fermi energy is adopted for the jellium electrodes and the electron transport at the zero bias limit is discussed in this paper. We use the local pseudopotentials described in Refs. 71 and 72 for the Na and Al ion-core potentials, respectively. For the exchange-correlations potential, we adopt the Ceperley-Alder form[73] parameterized by Perdew and Zunger.[74]

III. RESULTS

A. Al wire

We consider the three-Al-atom wire with triangular atomic bases between the jellium electrodes as shown in Fig. 1. We investigate bent, straight, and long wires, which are expressed by the displacement of the electrodes spacing Δd.

First, we show the bent and straight wires. Figure 2 shows conductance and channel transmissions at the Fermi energy as a function of Δd. The bond length b and atom-jellium distances are taken to be 5.4 and 2.6 bohrs, respectively. The center atom is displaced in the x direction, and the bond length is kept constant for the variation of Δd. The conductance increases with the increase in Δd. The fourth channel and higher channels have negligible values of less than 10^{-4}, which shows that only three channels contribute to the conduction of the wire. Compared with our previous results[69] without the triangular atomic bases, the conductance and
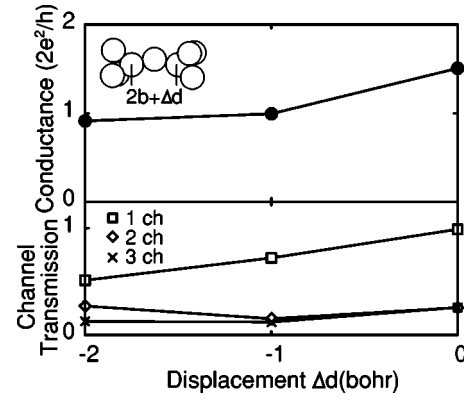

FIG. 2. Conductance (top) and channel transmissions (bottom) at the Fermi energy for three-Al-atom wires as a function of displacement of electrode spacing, Δd (fixed atom-atom bond length). For the atom bases contacting the jellium electrode, a triangular shape is used. (1 bohr$=0.529$ Å).

most of the channel transmissions are smaller. The conductance is less than the quantized unit for $\Delta d\leqslant-1$.

The character of the channels is elucidated using individual channel LDOS and channel current density. Throughout the paper we will plot the LDOS corresponding to the scattering states from the left at the Fermi energy. For the straight wire ($\Delta d=0$) shown in Fig. 3, the first channel has s, p_z, d_z^2, ..., orbital components ($l_z=0$) of Al atoms in
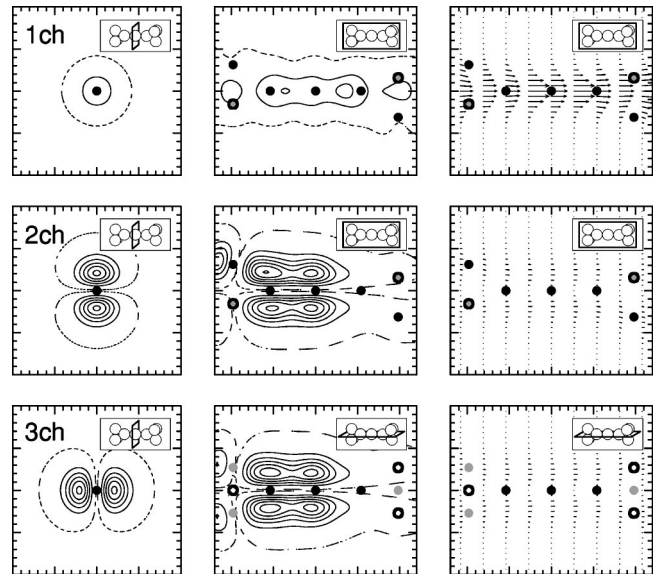

FIG. 3. Channel LDOS $[\rho^L_{E,n}(\boldsymbol{r})]$ and channel current density $[\boldsymbol{j}^L_{E,n}(\boldsymbol{r})]$ distributions at the Fermi energy for the straight three-Al-atom wires ($\Delta d=0$) with triangular bases. The states incident from the left electrode are shown. The top, middle, and bottom panels show the first, second, and third channels. The left and center panels show contours of the channel LDOS, and the right panels show arrows denoting the channel current density on the cross sections indicated in the inset panels. The contour spaces of the LDOS are taken as 2×10^{-2} hartree^{-1} bohr^{-3}. The broken lines correspond to 1×10^{-3} hartree^{-1} bohr^{-3}. The length of the arrows indicates the magnitude of the current density and the scale is the same in all panels. The solid black circles, the gray circles, and the open circles indicate the atomic positions on, under, and above the cross sections, respectively.
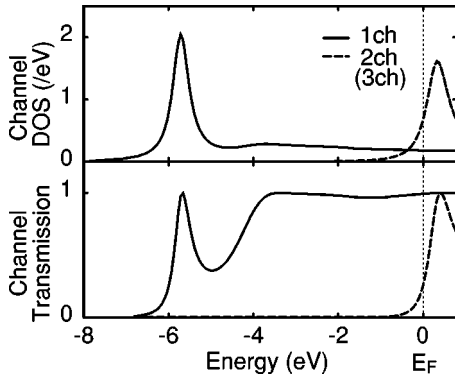
FIG. 4. Channel DOS around the center atom (top) and channel transmissions (bottom) for the straight Al atom wire as a function of the energy measured from the Fermi energy.

the wire. The second and third channels, which are degenerate, have p_x, d_{zx}, ..., and p_y, d_{zy}, ..., orbital components ($l_z = 1$). In this case, we call these channels s-p_z, p_x, and p_y channels since the contributions of s and p orbitals are dominant below the Fermi energy for the Al atom, although higher angular momentum components are automatically included with the plane wave basis set. Note that the LDOS distribution is symmetric with respect to the center atom only when the transmission is strictly unity.

The channel DOS around the center atom and the channel transmissions for the wire are shown in Fig. 4 as a function of the energy measured from the Fermi energy. The channel DOS is calculated by integrating the LDOS in the range of $z_a - b/2 < z < z_a + b/2$, z_a being the atomic position of the center atom and b the bond length. In an ideal one-dimensional system, the channel DOS has a sharp peak with a long tail on the higher energy side, $\sim 1/\sqrt{E}$, where the corresponding channel transmission saturates at unity. For the actual atomic wire, the onset of the band is smeared out with an additional resonancelike structure. The Fermi energy is located well above the onset energy of the first channel, but cuts just the smeared onset of the second and third channels. Therefore, the s-p_z channel is almost open, but the p_x and p_y channels are incompletely open at the Fermi energy. We point out here that the relation between the onset energies and the Fermi energy is important in terms of understanding the changes in transport properties with geometrical changes. Since the Fermi energy is located around the onset energy of the second and the third channel, the conductance is sensitive to geometrical changes of the Al wire.

For the bent wire ($\Delta d < 0$), the conduction channels are deformed, resulting in the lift of the degeneracy of the second and the third channels. Figure 5 shows the channel LDOS distributions at the Fermi energy for $\Delta d = -2$ bohrs. Due to the breaking of symmetry we can no longer observe the s-p_z or the p_x character of the first two channels around the central atom. Only the structure of the third channel, which has the character of a p_y orbital, is similar to that of the straight wire. The first and the second channels seem, however, to be orthogonal around the left atom to the center. We note that the first channel current forms a local loop current circulating the center atom, which may induce a magnetic moment.
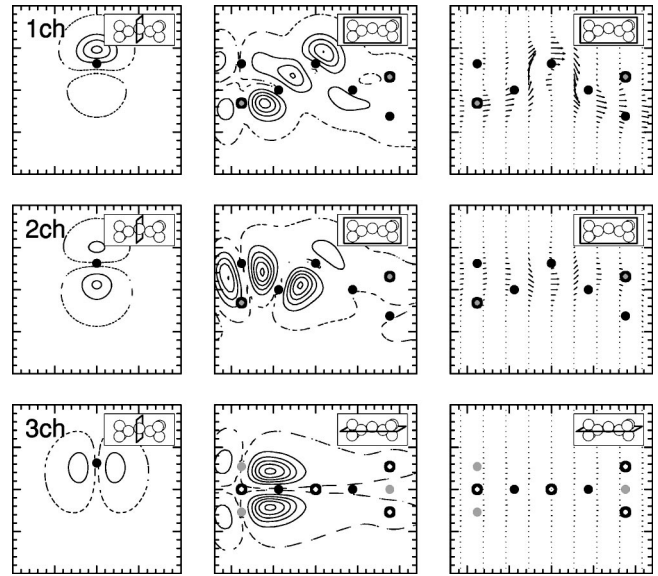

FIG. 5. Channel LDOS and channel current density distributions for the bent Al atom wires ($\Delta d = -2$ bohrs).

Figure 6 shows the channel DOS around the center atom and channel transmissions for $\Delta d = -2$ bohrs. The first channel of the straight wire is mixed with its second channel and the one-dimensional character weakens. Therefore, the first channel transmission at the Fermi energy has a smaller value than in the straight case. On the other hand, the second channel goes through a minimum for $\Delta d = -1$ bohrs but has almost the same transmission for $\Delta d = -2$ bohrs as in the straight configuration. The third decreases because of the slight upward shift of the channel onset energy relative to the Fermi energy. Thus, the conductance of the bent wire is smaller than that of the straight wire, and increases with the increase of Δd as shown in Fig. 2. Here we note that even though the conductance increases monotonously, not all channel transmissions increase. We will return to this point when we discuss the experimental data of the SNS junction.[55]

Next, we show the results for the longer wire corresponding to positive values of Δd. Figure 7 shows the conductance and channel transmissions as a function of Δd. The elongation of the right and left bonds of the central atom is assumed to be the same and is given by $\Delta d/2$. With the increase in bond length, the p_x and p_y channels close prior to the s-p_z channel, and the conductance decreases.
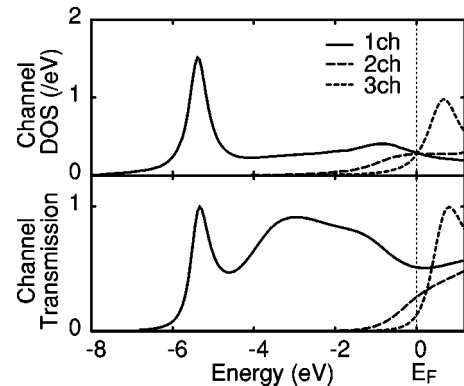

FIG. 6. Channel DOS around the center atom and channel transmissions for the bent Al atom wire ($\Delta d = -2$ bohrs).
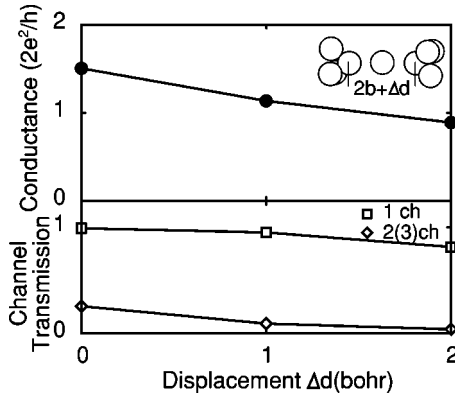
FIG. 7. Conductance and channel transmissions at the Fermi energy as a function of displacement of electrode spacing, Δd.

The conductance and the channel transmissions for a $\Delta d = 2$ bohrs are shown in Fig. 8. The overlap of wave functions between the atoms decreases, and the system becomes closer to a resonant tunneling regime. Therefore, the DOS and the transmissions have sharp peaks at the energies corresponding to the s and p orbitals of an Al atom. The Fermi energy is located below the sharp peaks in the DOS of the p_x and p_y channels. The second peak of the s-p_z channel, which mainly originates from the p_z orbital, is broadened due to the bonding to the neighboring atoms, and the Fermi energy located on the lower energy side of the peak. We confirmed that the resonant tunneling behavior is enhanced and a clearer second peak of the s-p_z channel is obtained with the further elongation of the bonds.

The character of the channels from the point of view of atomic orbitals is clearly seen in the channel LDOS and the channel current density at the resonance peaks as shown in Fig. 9, which shows their distributions at the resonance peak of the transmission of each channel: -5.27 and 2.23 eV of the first channel and 0.44 eV of the second and third channels. The first and the second peak of the first channel correspond to the s and p_z orbitals, and the first peaks of the second and the third channels to the p_x and p_y orbitals, respectively. In the resonant tunneling regime, each peak in the channel LDOS corresponds to an atomic orbital. However, note that an eigenchannel does not correspond to a single atomic orbital.
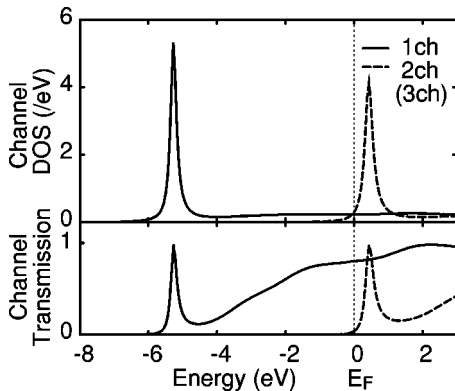

FIG. 8. DOS around the center atom and channel transmissions for the long Al atom wires ($\Delta d = 2$ bohrs) as a function of the energy measured from the Fermi energy.
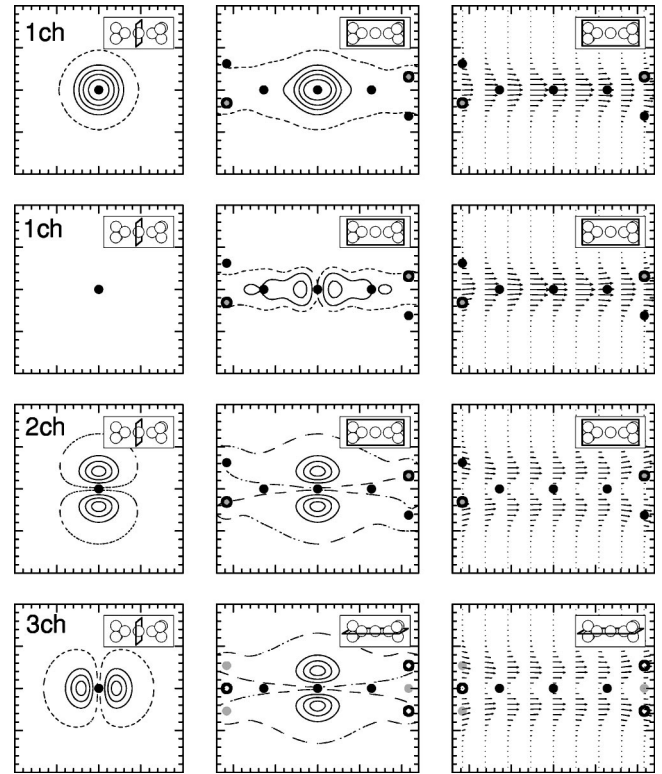

FIG. 9. Channel LDOS and current density distributions for the Al atom wires for the $\Delta d = 2$ bohrs. The two upper panels correspond to the first and the second resonance peak of the first channel, respectively. The first panel in the second row corresponds to a nodal plane. The two bottom panels correspond to the first peak of the second and the third channels. The broken lines correspond to the 0.01 hartree^{-1} bohr^{-3}. The contour spaces are 0.02 hartree^{-1} bohr^{-3} for the second panel and 0.2 hartree^{-1} bohr^{-3} for the other panels, respectively.

B. Na wire

Figure 10 (top) shows the conductance as a function of the displacement of the electrode spacing, Δd, of the three-atom-long Na wire with a rectangular configuration of the atomic bases contacting the jellium electrodes. The atom-atom and atom-jellium distances are taken to be 7 and 3
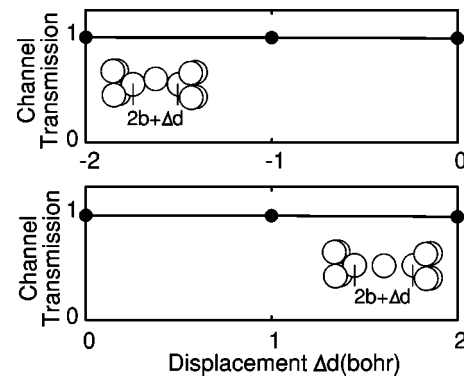

FIG. 10. First channel transmissions (conductance in unit of G_0) for three-atom-long Na wires with rectangular atom bases contacting the jellium electrodes. The top and the bottom panels show the transmissions as a function of displacement of electrode spacing, Δd.
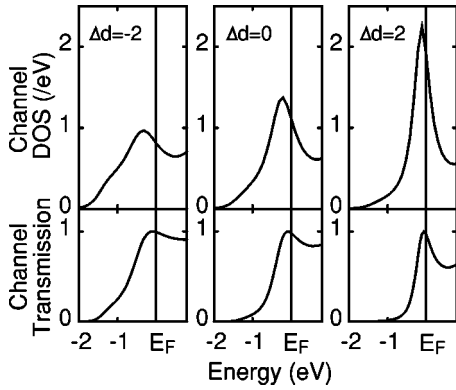
FIG. 11. Channel DOS around the center atom and channel transmissions of the Na wires as a function of the energy measured from the Fermi energy. The left, middle, and right panels correspond to bent, straight, and long ($\Delta d = -2, 0, 2$ bohrs) wires, respectively.
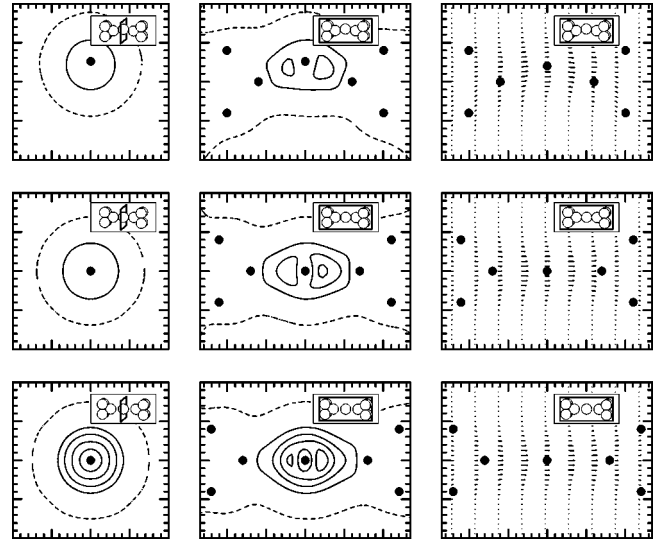

FIG. 12. Channel LDOS and channel current density distributions for bent (top), straight (middle), and long (bottom) Na atom wires. The contour spaces of the LDOS are taken as 2×10^{-2} hartree^{-1} bohr^{-3}. The broken lines correspond to 1×10^{-3} hartree^{-1} bohr^{-3}.

bohrs, respectively. The conductance is very close to one quantum unit and is insensitive to bending, in contrast to that of the Al wire. Except for one open channel, all channel transmissions are negligible with transmissions of less than 10^{-3}. Thus, a single channel contributes to the transport through the wire. The conductance of the long Na wire is also shown in Fig. 10 (bottom). As in the case of bent wire, the single channel transmits electrons through the long wire, and the conductance has only a slight decrease from the quantum value.

As in the case of Al, the behavior of the transmission can be explained by the position of the Fermi energy relative to the onset of the channel. For the straight and bent wires, as shown in Fig. 11, the Fermi energy cuts above the onset of the conduction channel, where it shows a smeared-out one-dimensional character. The state of the channel does not change significantly and the conductance is insensitive to bending. Consequently, the conductance shows the quantized value. For the long wire, the Fermi energy cuts very close to the resonant peak of the s orbital of the Na atom, since the orbital contains a single electron. Thus, the conductance also shows the quantized value for the case of the long wire.

Figure 12 shows the channel LDOS distributions of the Na atom wire. A clear s character is seen with a slight distortion for the bent wire and with an increase in density for the long wire.

IV. DISCUSSION

It is a special feature of the Al contacts that three open channels contribute to the transport and that the steps of the conductance staircase have positive slopes: the conductance increases as the contacts are elongated. Experimentally, using the MCB technique with a SNS junction, the number of channels of the single Al atom contacts and the channel transmissions during the elongation processes were measured.[55,56] Just before the contact breaks, three channels contribute to the transport through the contact, and the transmission of one of these channels is much larger than others. The positive slopes were observed clearly in the MCB and the STM experiments.[7,40,62]

The Al single atom contact has already been analyzed

theoretically by Lang[50] using the first-principles approach. However, thus far the conduction channels of the Al contacts have only been analyzed using a tight-binding model.[61] The tight-binding results showed three contributing channels of the wire in agreement with the present results and with the experimental results. This is also consistent with the free electron approach for the valence number of 3.[60] Although the one channel is almost open for the straight wire, all channels are sensitive to geometrical changes, and incomplete open channels emerge even for a slightly disordered structure. In actual contacts, particularly at low temperature, not well ordered structures are often formed, and then incomplete open channels are expected to be observed.

Regarding the positive slope, the first-principles method[40] was able to account for the effect in the case of larger contacts: The physical origin was related to the change in the bulk band structure under high uniaxial strain. For the atomic-scale Al contacts, the calculation using a tight binding model[62] suggested that the reason for the positive slope was the changes of the states in the contact with the elongation of the bonds. In this case, all three channel transmissions increased with the elongation. In contrast to that result, our results for the atomic-scale contacts suggest that the reason is stretching of disordered bent structures towards a straight structure with the pulling of the contact, rather than the bond elongation effect. In our calculation, the Fermi energy is not located at the center of the resonant peak of the p_z orbital but rather in the lower energy tail of the peak for the longer bond wire. We have confirmed that this is the same for the case where the narrowest part of the contact is formed by a single atom. Therefore, we find that the individual transmissions and the conductance decrease with the increase in the bond length.

The experimental values of the gradient of the conductance slope immediately before the contact breaks are estimated as $0.1-1 G_0/\text{Å}$ (depending on the data) in Ref. 62 and $0.01 G_0/\text{Å}$ in Ref. 40. Our calculated gradients of the con-

ductance $(\Delta G)/(\Delta d)$ is $0.16G_0/\text{Å}$ $(-2<\Delta d<-1)$ and $0.97G_0/\text{Å}$ $(-1<\Delta d<0)$, which are in good agreement with the former experimental data and larger than the latter. The slope is likely to change from one pull to another depending on the exact geometry of the contacts. If the structure changes do not occur at the narrowest point, which is controlling the conductance, we expect a lower value for the slope. Thus, the fact that our theoretical estimate is larger than the latter experimental values is to be expected.

Our calculated gradients of the channel transmissions $(\Delta T_i)/(\Delta d)$ are 0.40, –0.23, –0.01 $(/\text{Å})$ $(i=1,2,3)$ for $-2<\Delta d<-1$, and 0.51, 0.20, 0.26 $(/\text{Å})$ $(i=1,2,3)$ for $-1<\Delta d<0$. Note that not all of the gradients are positive. The experimental data measured during elongation of the SNS contacts show that the lower channel transmissions decrease when the largest channel transmission (and the conductance) increase.[55] Our results agree well with this observation, which is not explained by the tight-binding model.[61] The experimental data also show that the three channel transmissions decrease just before the tunneling regime. At that moment the bonds are expected to be elongated. Our calculated results show that conductance and three channel transmissions decrease when the bonds are elongated. The calculated gradients of the transmissions are –0.076, –0.31 $(/\text{Å})$ $[i=1,2(3)]$ for $0<\Delta d<1$, and –0.26, –0.10 $(/\text{Å})$ $[i=1,2(3)]$ for $1<\Delta d<2$. We considered the system where the two bonds of the center atom were elongated, but we have also confirmed that the situation is the same for the case where only a single bond on one side is elongated.

For the Na atomic contacts, the experiments show clear quantized conductance during the elongation process.[8] As described in Sec. III, the calculated results show that a single open channel contributes to the transport through a single Na atom wire, and that the conductance is stable against small changes in the geometry. The gradients of the conductance slope are -0.0095, -0.0076, -0.0076, and -0.021 $G_0/\text{Å}$ for $-2<\Delta d<-1$, $-1<\Delta d<0$, $0<\Delta d<1$, and $1<\Delta d<2$, respectively, which are much smaller than for the Al wires. This explains why stable quantized conductance plateaus are clearly observed in the experiments although the atomic configurations are changing in the elongation processes. This is in agreement with the recent calculation of the conductance combined with the molecular dynamics simulation by Nakamura and co-workers.[64]

The difference in values of the conductance of the Na wire obtained by Lang's calculation,[51] which shows a lower conductance than the quantized unit, is explained by the different density of the jellium electrodes. The valence electron density of an alkali metal such as Na is much smaller than that of other materials. Therefore, we take $r_s=4$ bohrs for the jellium electrodes, which corresponds to the average density of bulk Na. This reduces the charge transfer between the jellium and atomic wires, and the artificial reflections at the connections to the jellium. Particularly, without the atom bases between the wire and the jellium electrodes, the difference is distinct. For the high density case of $r_s=2$ bohrs, corresponding to the calculation by Lang, the oscillations of the transmission are enhanced due to multiple reflections between the two connections to the jellium electrodes. The conductance is smaller than the quantized value because the Fermi energy is located on the higher energy side of the pronounced first peak.

V. CONCLUSION

We have presented a first-principles method for investigating electron transport, in particular, conduction channels through atomic wires. We have elucidated the nature of the channels through Al and Na monatomic wires. In terms of the decomposition of the LDOS and the current density into eigenchannels, the details of the conduction channels were described. Three channels contribute to the transport through the Al atom wire, whose channel transmissions are sensitive to geometrical changes (bending and elongation of bonds). The conductance increases with bending towards a straight configuration. With further elongation of the bond, two channels close and the conductance decreases. Our calculations can explain the positive slopes found for the conductance plateaus of single atom Al contacts: a bent wire stretches towards a straight configuration during the pulling of the contact while the Al-Al bond lengths remain almost constant. Furthermore, the stretching process can also explain the decrease of some of the channel transmissions during the increase of the conductance. In contrast to these results, we find for the Na atom wire only a single fully open channel. The conductance showing the quantized value is stable against small geometrical changes.

ACKNOWLEDGMENTS

[1] G. Binnig, H. Rohrer, Ch. Gerber, and E. Weibel, Phys. Rev. Lett. **49**, 57 (1982).

[2] C.J. Muller, J.M. van Ruitenbeek, and L.J. de Jongh, Physica C **191**, 485 (1992).

[3] N. Agraït, J.G. Rodrigo, and S. Vieira, Phys. Rev. B **47**, 12 345 (1993).

[4] N. Agraït, G. Rubio, and S. Vieira, Phys. Rev. Lett. **74**, 3995 (1995).

[5] G. Rubio, N. Agraït, and S. Vieira, Phys. Rev. Lett. **76**, 2302 (1996).

[6] C. Untiedt, G. Rubio, S. Vieira, and N. Agraït, Phys. Rev. B **56**, 2154 (1997).

[7] J.M. Krans, C.J. Muller, I.K. Yanson, Th.C.M. Govaert, R. Hesper, and J.M. van Ruitenbeek, Phys. Rev. B **48**, 14 721 (1993).

[8] J.M. Krans, J.M. van Ruitenbeek, V.V. Fisun, I.K. Yanson, and L.J. de Jongh, Nature (London) **375**, 767 (1995).

[9] C.J. Muller, J.M. Krans, T.N. Todorov, and M.A. Reed, Phys. Rev. B **53**, 1022 (1996).

[10] A.I. Yanson and J.M. van Ruitenbeek, Phys. Rev. Lett. **79**, 2157 (1997).

[11] A.I. Yanson, G.R. Bollinger, H.E. van den Brom, N. Agraït, and J.M. van Ruitenbeek, Nature (London) **395**, 783 (1998).

[12] J.I. Pascual, J. Méndez, J. Gómez-Herrero, A,M. Baró, N. García, and Vu Thien Binh, Phys. Rev. Lett. **71**, 1852 (1993).

[13] J.I. Pascual, J. Méndez, J. Gómez-Herrero, A,M. Baró, N. García, Uzi Landman, W.D. Luedtke, E.N. Bogachek, and H.-P. Cheng, Science **267**, 1793 (1995).

[14] L. Olesen, E. Lægsgaard, I. Stensgaard, F. Besenbacher, J. Schiøtz, P. Stoltze, K.W. Jacobsen, and J.K. Nørskov, Phys. Rev. Lett. **72**, 2251 (1994).

[15] M. Brandbyge, J. Schiøtz, M.R. Sørensen, P. Stoltze, K.W. Jacobsen, J.K. Nørskov, L. Olesen, E. Lægsgaard, I. Stensgaard, and F. Besenbacher, Phys. Rev. B **52**, 8499 (1995).

[16] K. Hansen, E. Lægsgaard, I. Stensgaard, and F. Besenbacher, Phys. Rev. B **56**, 2208 (1997).

[17] J.L. Costa-Krämer, N. Garcia, P. Garcia-Mochales, and P.A. Serena, Surf. Sci. **342**, L1144 (1995).

[18] J.L. Costa-Krämer, N. Garcia, P. Garcia-Mochales, P.A. Serena, M.I. Marqués, and A. Correia, Phys. Rev. B **55**, 5416 (1997).

[19] J.L. Costa-Krämer, Phys. Rev. B **55**, R4875 (1997).

[20] J.L. Costa-Krämer, N. Garcia, and H. Olin, Phys. Rev. Lett. **78**, 4990 (1997).

[21] J.L. Costa-Krämer, N. Garcia, and H. Olin, Phys. Rev. B **55**, 12 910 (1997).

[22] D.P.E. Smith, Science **269**, 371 (1995).

[23] C. Sirvent, J.G. Rodrigo, S. Vieira, L. Jurczyszyn, N. Mingo, and F. Flores, Phys. Rev. B **53**, 16 086 (1996).

[24] Z. Gai, Y. He, H. Yu, and W.S. Yang, Phys. Rev. B **53**, 1042 (1996).

[25] H. Yasuda and A. Sakai, Phys. Rev. B **56**, 1069 (1997).

[26] K. Itakura, K. Yuki, S. Kurokawa, H. Yasuda, and A. Sakai, Phys. Rev. B **60**, 11 163 (1999).

[27] H. Ohnishi, Y. Kondo, and K. Takayanagi, Nature (London) **395**, 780 (1998).

[28] H. Oshima and K. Miyano, Appl. Phys. Lett. **73**, 2203 (1998).

[29] C.Z. Li, H. Sha, and N.J. Tao, Phys. Rev. B **58**, 6775 (1998).

[30] T. Ono, Y. Ooka, H. Miyajima, and Y. Otani, Appl. Phys. Lett. **75**, 1622 (1999).

[31] W.B. Jian, C.S. Chang, W.Y. Li, and T.T. Tsong, Phys. Rev. B **59**, 3168 (1999).

[32] B.J. van Wees, H. van Houten, C.W.J. Beenakker, J.G. Williamson, L.P. Kouwenhoven, D. van der Marel, and C.T. Foxon, Phys. Rev. Lett. **60**, 848 (1988).

[33] D.A. Wharam, T.J. Thornton, R. Newbury, M. Pepper, H. Ahmed, J.E.F. Frost, D.G. Hasko, D.C. Peacock, D.A. Ritchie, and G.A.C. Jones, J. Phys. C **21**, L209 (1988).

[34] T.N. Todorov and A.P. Sutton, Phys. Rev. Lett. **70**, 2138 (1993).

[35] A.M. Bratkovsky, A.P. Sutton, and T.N. Todorov, Phys. Rev. B **52**, 5036 (1995).

[36] J.A. Torres, J.I. Pascual, and J.J. Sáenz, Phys. Rev. B **49**, 16 581 (1994).

[37] J.A. Torres and J.J. Sáenz, Phys. Rev. Lett. **77**, 2245 (1996).

[38] A. García-Martín, J.A. Torres, and J.J. Sáenz, Phys. Rev. B **54**, 13 448 (1996).

[39] J.I. Pascual, J.A. Torres, and J.J. Sáenz, Phys. Rev. B **55**, 16 029 (1997).

[40] D. Sánchez-Portal, C. Untiedt, J.M. Soler, J.J. Sáenz, and N. Agraït, Phys. Rev. Lett. **79**, 4198 (1997).

[41] H. Mehrez, S. Ciraci, A. Buldum, and I.P. Batra, Phys. Rev. B **55**, R1981 (1997).

[42] H. Mehrez and S. Ciraci, Phys. Rev. B **56**, 12 632 (1997).

[43] U. Landman, W.D. Luedtke, B.E. Salisbury, and R.J. Colton, Phys. Rev. Lett. **77**, 1362 (1996).

[44] R.N. Barnett and U. Landman, Nature (London) **387**, 788 (1997).

[45] J.M. van Ruitenbeek, M.H. Devoret, D. Esteve, and C. Urbina, Phys. Rev. B **56**, 12 566 (1997).

[46] P. García-Mochales and P.A. Serena, Phys. Rev. Lett. **79**, 2316 (1997).

[47] C.C. Wang, J.L. Mozos, G. Taraschi, J. Wang, and H. Guo, Appl. Phys. Lett. **71**, 419 (1997).

[48] A. Levy Yeyati, A. Martín-Rodero, and F. Flores, Phys. Rev. B **56**, 10 369 (1997).

[49] E. Bascones, G. Gómez-Santos, and J.J. Sáenz, Phys. Rev. B **57**, 2541 (1998).

[50] N.D. Lang, Phys. Rev. B **52**, 5335 (1995).

[51] N.D. Lang, Phys. Rev. Lett. **79**, 1357 (1997).

[52] N.D. Lang and Ph. Avouris, Phys. Rev. Lett. **81**, 3515 (1998).

[53] N.D. Lang and Ph. Avouris, Phys. Rev. Lett. **84**, 358 (2000).

[54] H. Imamura, N. Kobayashi, S. Takahashi, and S. Maekawa, Phys. Rev. Lett. **84**, 1003 (2000).

[55] E. Scheer, P. Joyez, D. Esteve, C. Urbina, and M.H. Devoret, Phys. Rev. Lett. **78**, 3535 (1997).

[56] E. Scheer, N. Agraït, J.C. Cuevas, A.L. Yeyati, B. Ludoph, A. Martí-Rodero, G.R. Bollinger, J.M. van Ruitenbeek, and C. Urbina, Nature (London) **394**, 154 (1998).

[57] M. Büttiker, IBM J. Res. Dev. **32**, 63 (1988).

[58] M. Brandbyge and K. W. Jacobsen, in *Nanowires*, edited by P. A. Serena and N. García (Kluwer Academic, Dordrech, 1997), p. 61.

[59] M. Brandbyge, M.R. Sørensen, and K.W. Jacobsen, Phys. Rev. B **56**, 14 956 (1997).

[60] T. López-Ciudad, A. García-Martín, A.J. Caamaño, and J.J. Sáenz, Surf. Sci. **440**, L887 (1999).

[61] J.C. Cuevas, A. Levy Yeyati, and A. Martín-Rodero, Phys. Rev. Lett. **80**, 1066 (1998).

[62] J.C. Cuevas, A. Levy Yeyati, A. Martín-Rodero, G.R. Bollinger, C. Untiedt, and N. Agraït, Phys. Rev. Lett. **81**, 2990 (1998).

[63] M. Brandbyge, N. Kobayashi, and M. Tsukada, Phys. Rev. B **60**, 17 064 (1999).

[64] A. Nakamura, M. Brandbyge, L.B. Hansen, and K.W. Jacobsen, Phys. Rev. Lett. **82**, 1538 (1999).

[65] H. Häkkinen, R.N. Barnett, and U. Landman, J. Phys. Chem. B **103**, 8814 (1999).

[66] N. Kobayashi, M. Brandbyge, and M. Tsukada, Jpn. J. Appl. Phys., Part 1 **38**, 336 (1999).

[67] K. Hirose and M. Tsukada, Phys. Rev. Lett. **73**, 150 (1994); Phys. Rev. B **51**, 5278 (1995);

[68] N. Kobayashi and M. Tsukada, Jpn. J. Appl. Phys., Part 1 **38**, 3805 (1999).

[69] N. Kobayashi, M. Brandbyge, and M. Tsukada, Surf. Sci. **433-435**, 854 (1999).

[70] W. Kohn and L.J. Sham, Phys. Rev. **140**, A1133 (1965).

[71] N.W. Ashcroft, Phys. Lett. **23**, 48 (1966).

[72] M. Schlüter, J.R. Chelikowsky, S.G. Louie, and M.L. Cohen, Phys. Rev. B **12**, 4200 (1975).

[73] D.M. Ceperley and B.J. Alder, Phys. Rev. Lett. **45**, 566 (1980).

[74] J.P. Perdew and A. Zunger, Phys. Rev. B **23**, 5048 (1981).